



Optical and structural properties of Si nanocrystals produced by Si hot implantation

U. S. Sias, M. Behar, H. Boudinov, and E. C. Moreira

Citation: *Journal of Applied Physics* **102**, 043513 (2007); doi: 10.1063/1.2772500

View online: <http://dx.doi.org/10.1063/1.2772500>

View Table of Contents: <http://scitation.aip.org/content/aip/journal/jap/102/4?ver=pdfcov>

Published by the [AIP Publishing](#)



Re-register for Table of Content Alerts

Create a profile.



Sign up today!



Optical and structural properties of Si nanocrystals produced by Si hot implantation

U. S. Sias^{a)}

Centro Federal de Educação Tecnológica de Pelotas (CEFET-RS), 96015-370, Pelotas-RS, Brazil

M. Behar and H. Boudinov

Instituto de Física - Universidade Federal do Rio Grande do Sul (UFRGS), C.P. 15051, 91501-970 Porto Alegre-RS, Brazil

E. C. Moreira

UFPEL – UNIPAMPA, Campus Bagé, 96400-970, Bagé-RS, Brazil

(Received 26 February 2007; accepted 6 July 2007; published online 22 August 2007)

It was already demonstrated that Si hot implantation followed by high-temperature annealing induces the formation of Si nanocrystals (Si NCs) which when excited in a linear excitation regime present two photoluminescence (PL) bands (at 780 and 1000 nm). We have undertaken the present work in order to investigate three features: First, to determine the origin of each band. With this aim we have changed the implantation fluence and the high-temperature annealing time. Second, to investigate the influence of the postannealing atmosphere on the PL recovering process after bombarding the Si NCs. Third, we have annealed the as-produced Si NCs in a forming gas (FG) atmosphere in order to observe the PL behavior of each band. The results have shown that the 780 nm PL band has its origin in radiative interfacial states, while the 1000 nm one is due to quantum size effects. From the experiments we have concluded that the PL recovery after the Si NCs irradiation strongly depends on the type of postannealing atmosphere. Finally, it was found that the FG treatment strongly affects the line shape of the PL spectrum. © 2007 American Institute of Physics. [DOI: [10.1063/1.2772500](https://doi.org/10.1063/1.2772500)]

I. INTRODUCTION

Since the discovery of light emission in porous Si¹ and in Si nanocrystallites,^{2,3} an intense research activity has been developed in studying Si nanostructures due to their promising applications in optoelectronics and photonic devices.^{4–6} The investigation of structures consisting of Si nanocrystals (Si NCs) has been mostly devoted to improving their quantum efficiency for photoluminescence (PL), as well to understanding their light absorption and emission processes. Although the exact mechanism for light emission remains controversial, nowadays it is well established that basically it relies either on NC size effects^{7–9} or on radiative processes at the Si NCs/matrix interface.^{9–12}

Several techniques have been used to produce Si NCs embedded in a SiO₂ matrix, among them chemical vapor deposition (CVD), molecular beam epitaxy (MBE), laser ablation, and in particular the ion implantation technique. This last one has been used quite frequently because it has several advantages. In addition to its compatibility with the microelectronic technology, it is very reproducible concerning the depth where the ions are deposited, as well as the Si excess induced by the implantation.

The properties of the Si NCs produced by ion implantation in a SiO₂ matrix have been extensively studied as a function of the implantation fluence, annealing temperature, and annealing time.^{10,13–15} However, in all the previous works the implantation has been performed at room tempera-

ture (RT) and only one PL band centered at 780 nm was observed, in agreement with results obtained using the other techniques mentioned (CVD, MBE, etc).

More recently, we have taken another experimental approach in order to form the Si NCs. Instead of performing the Si implantation at RT, we have done it at temperatures between 400 and 800 °C followed by annealing at high temperature ($T > 1100$ °C). The implantation was performed with a fluence of $\Phi = 1 \times 10^{17}$ Si/cm², the PL spectra being obtained in a linear excitation regime (power density of 20 mW/cm²), a very important feature, as was previously discussed in the literature.¹⁶ Consequently we have observed two PL bands, the first centered at $\lambda = 780$ nm and the second and new one, with higher intensity, at λ around 1000 nm. Transmission electron microscopy (TEM) measurements revealed that the hot implanted samples have a larger and broader Si NC distribution than the ones implanted at RT. Since the origin of these two PL bands is not clear, the first objective of the present work is to answer this question.

It was shown that the PL induced by the Si NCs is quenched after Si irradiation as a consequence of the nanocrystal amorphization. However, it is fully recovered when a high-temperature postannealing (temperatures between 800 and 1100 °C) is performed.¹⁷ In the present case the appearance of two PL bands as a consequence of the Si hot implantations raises two interesting questions that deserve investigation. First, what would the behavior of both PL bands be after irradiation and further annealing? Second, should the annealing atmosphere affect the PL recovery?

^{a)}Electronic mail: uilson@cefetrst.tche.br

One final question should be raised. It is well known that a thermal treatment at relatively low temperature (around 500 °C) in a forming gas (FG) atmosphere passivates the Si dangling bonds at the nanocrystal surface, bringing as a consequence an increase of the PL intensity induced by the Si NCs.^{18–21} Then, the appearance of two PL bands raises the following questions: (a) Is the passivation effect similar for both bands? (b) When the preannealing time is changed, how does it affect further FG treatment?

In order to answer the above questions, we have undertaken the present work, which was divided in three parts. In the first one we studied the influence of the implanted fluence and annealing time on the behavior of both bands and, consequently, tried to identify their origin. In the second one, after forming the nanocrystals we bombarded them, quenched the PL emission, and then postannealed the samples in N₂ or Ar atmosphere, studying the PL recovery as a function of the annealing time and atmosphere. Finally, for a given implantation fluence we have submitted the samples to several preannealing times (at 1100 °C), then performed the FG treatment and observed the behavior of both PL bands.

II. EFFECT OF THE IMPLANTATION FLUENCE AND ANNEALING TIME ON THE PL BEHAVIOR

A. Experimental procedure

A 480 nm thick SiO₂ layer thermally grown onto a Si (100) wafer was implanted with 170 keV Si ions at fluences of $\Phi=0.35, 0.5, 1.0, 2.0, 3.0,$ and 4.0×10^{17} at/cm², keeping the substrate at 600 °C. Some samples were implanted at RT. Consequently, we have obtained Si excess concentrations in a range between 3 and 40 at % at around 250 nm depth. The samples were further annealed at 1100 °C for 1 h in a N₂ atmosphere in order to form the Si NCs. We have also investigated the effect of the annealing time (between 1 and 15 h) on the samples implanted with $\Phi=1 \times 10^{17}$ Si/cm². PL measurements were performed at RT using a Xe lamp with a monochromator, in order to get a wavelength of 488 nm as an excitation source. The emission was dispersed by a 0.3 m single-grating spectrometer and collected with a visible near-infrared Si detector and an InGaAs cooled one. All spectra were obtained under the same conditions and corrected for the system response.

The structural characterization was performed by using TEM measurements in a 200 keV JEOL microscope with the samples prepared in a cross-sectional geometry.

B. Results

Figure 1 shows the PL spectra of samples implanted with Si fluences between 0.35×10^{17} and 4×10^{17} Si/cm² and postannealed at 1100 °C for 1 h. The inset of this figure illustrates details of the PL region corresponding to the $650 \leq \lambda \leq 950$ nm wavelength interval. An inspection of the figure shows several interesting features. First, for the lowest implantation fluence only the band centered at 780 nm appears. Second, the shape of the PL spectra changes drastically by increasing the implanted Si fluence. In fact, for fluences higher than 0.5×10^{17} Si/cm² two PL bands can be

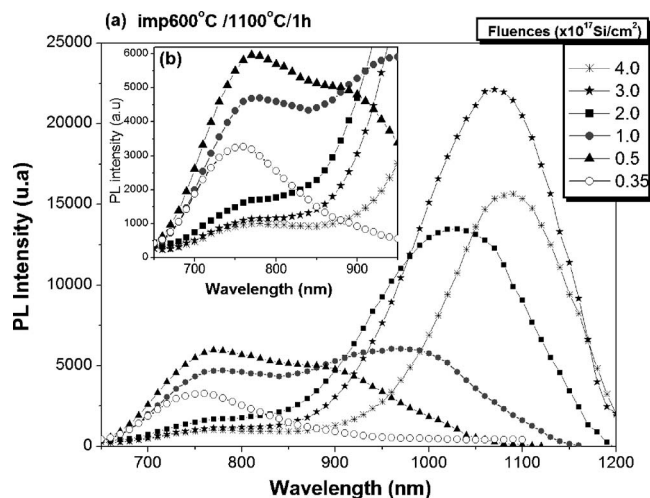


FIG. 1. (a) Typical PL spectra of samples implanted at 600 °C with different fluences and subsequently annealed at 1100 °C/1 h. (b) Inset corresponds to the spectra shown in (a), expanded in the wavelength region of 650–950 nm.

distinguished clearly: one centered at 780 nm and a new one at around 1000 nm. The first PL band increases its intensity with the fluence up to $\Phi=0.5 \times 10^{17}$ Si/cm² and then decreases without shifting its position – see inset. On the other hand, the second PL band ($\lambda \sim 1000$ nm) increases its PL signal continuously up to $\Phi=3 \times 10^{17}$ Si/cm² and then decreases, showing a strong redshift with the increasing implanted fluence.

We have fitted the PL spectra with two Gaussians in order to quantify the intensities of both PL bands and their positions. It should be stressed that this is an empirical procedure that, in all the cases, has reproduced in a unique way the experimental results. Consequently, Fig. 2 shows that the band centered at $\lambda=780$ nm slightly changes the intensity (I_1), but not its position (λ_1), which remains almost constant with the implantation fluence.

Therefore, in what follows, we will concentrate our attention on the behavior of the long wavelength band. Figure 2(a) displays the evolution of the PL peak intensity (I_2) of this band as a function of the implanted fluence. As quoted above, it increases its intensity with the fluence reaching a maximum at $\Phi=3 \times 10^{17}$ Si/cm² and then decreases by 30% for the highest implanted fluence. Concerning the PL peak position (λ_2), it suffers a noticeable redshift with increasing fluence, changing from 850 to around 1100 nm—see Fig. 2(b).

Figure 3 shows some typical dark-field images from the TEM observations. Figures 3(a) and 3(b) illustrate images from samples that were implanted at the same temperature (600 °C) but with different fluences (2×10^{17} and 4×10^{17} Si/cm²). On the other hand, Figs. 3(b) and 3(c) show images from samples implanted with the same fluence (4×10^{17} Si/cm²), but at different implantation temperatures, 600 °C and RT, respectively. In all the cases, the Si NCs size distributions have shown Gaussian profiles, as illustrated in Fig. 4.

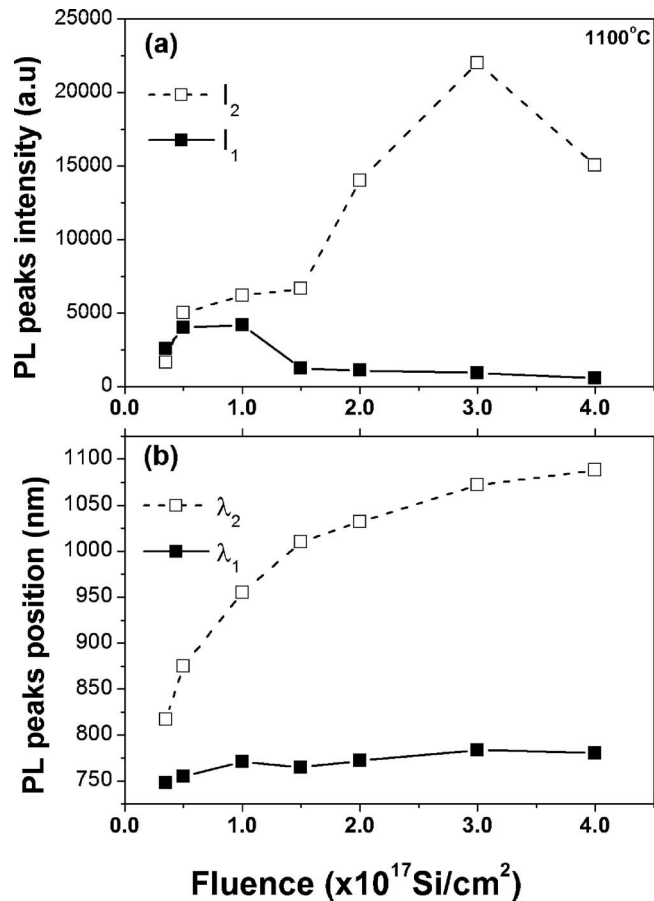


FIG. 2. (a) PL peak intensities and (b) positions as a function of the fluence for samples implanted at 600 °C and annealed at 1100 °C/1 h. I_1 and I_2 represent the peak intensities for the short and the long wavelength PL bands centered at the positions λ_1 and λ_2 , respectively.

Figure 5 summarizes the structural information from the TEM results. As can be observed, the Si NC mean size and size distribution have a straight dependence with the implanted fluence and implantation temperature. An inspection of the figure shows two features: First, the hot implanted samples always present larger nanocrystals with a broader size distribution as compared with those produced by RT implantations. Second, in both cases the mean size and size distribution are strongly dependent on the implanted fluence.

Finally, it should be stressed that even implantations performed at 800 °C, without the postannealing step at $T > 1100$ °C, does not induce Si NCs formation as revealed by TEM observations.

Concerning the PL evolution with the annealing time, we have performed experiments with samples implanted at 600 °C at a fluence of $\Phi = 1 \times 10^{17}$ Si/cm² and postannealed at 1100 °C. As illustrated in Fig. 6, while the first PL band ($\lambda = 780$ nm) does not reveal any noticeable change, the second one ($\lambda \cong 1000$ nm) shows a strong dependence with the annealing time. In Fig. 6(a) it can be observed that the PL intensity increases with the annealing time, but after 6 h it tends to saturate. Figure 6(b) plots the respective peak position as a function of the annealing time, which shows a red-shift evolution followed by a tendency to saturation after 6 h. This is the same kind of behavior as that observed in Fig. 6(a).

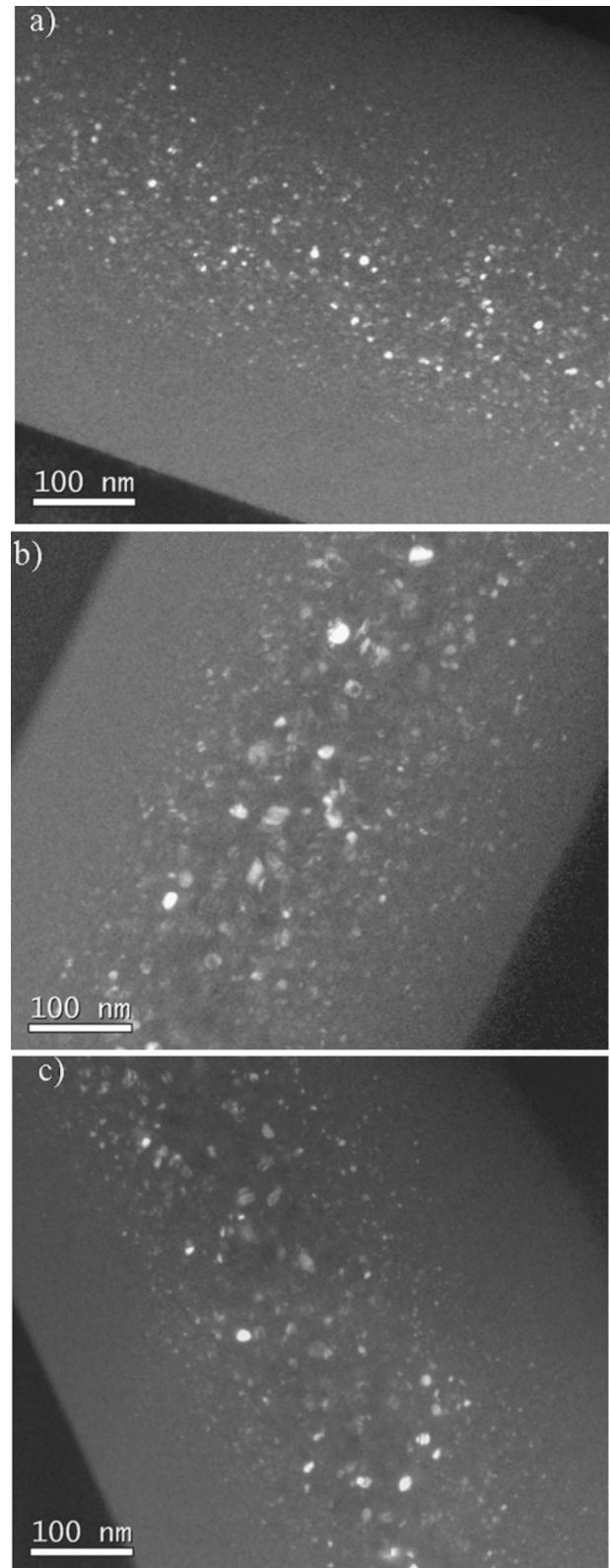


FIG. 3. Cross-sectional TEM images in dark-field contrast from samples implanted, respectively, at the following fluences and temperatures: (a) 2×10^{17} Si/cm² at 600 °C; (b) 4×10^{17} Si/cm² at 600 °C; and (c) 4×10^{17} Si/cm² at RT. These samples were subsequently annealed at 1100 °C/1 h.

C. Discussion and conclusions

The results of the present study, performed by Si implantations with the SiO₂ substrate kept at 600 °C, are at vari-

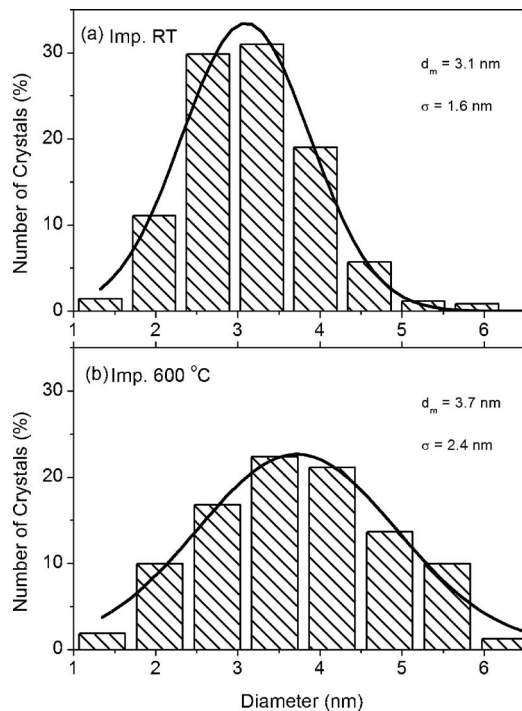


FIG. 4. Typical Gaussian fittings of size histograms from TEM analyses. (a) Sample implanted at RT and (b) sample implanted at 600 °C. Both samples were implanted with a fluence of 1×10^{17} Si/cm² and annealed at 1100 °C/1 h.

ance with what was previously published in the literature for RT implantations. For the lowest implantation fluence we have basically observed one PL band centered at 780 nm. This feature could be attributed to the low excess Si in the matrix (3.5 at %). However, for fluences higher than $\Phi = 0.5 \times 10^{17}$ Si/cm², a second PL band clearly appears, with higher intensity and centered at around 1000 nm, which was never observed before. Regarding the behavior of the 780 nm PL band, its intensity slightly changes with the implantation fluence, but its position is almost independent of the Si excess concentration. Previous works on Si NCs produced by RT Si implantations in SiO₂ matrix have only reported the existence of a single PL band around 780 nm. The absence of a PL redshift for this band with increasing fluences was observed in Ref. 3 in contrast with the results of Refs. 10 and 13, where a PL redshift with the fluence was reported. Our results are clearly in agreement with those of Ref. 3, since no change in the 780 nm PL position was observed. These contradictory results could be due to nonlinear effects in the PL emission produced by the use of high laser excitation power densities on the samples, as we have previously demonstrated.¹⁶ Thus, concerning the 780 nm (~ 1.6 eV) band, it can be attributed to radiative states at the Si/SiO₂ interface.

The origin of the 780 nm PL band can be explained on the following basis. There are in the literature *ab initio* calculations^{22,23} indicating that oxygen atoms at the interface Si/SiO₂ can act as charge trapping centers by shrinking the band gap below the Si NC one. Then, radiative recombination of electrons, holes, and excitons could take place in this region. This effect has been shown to be more pronounced for Si NCs with smaller diameters (< 2 nm).²⁴ All carriers

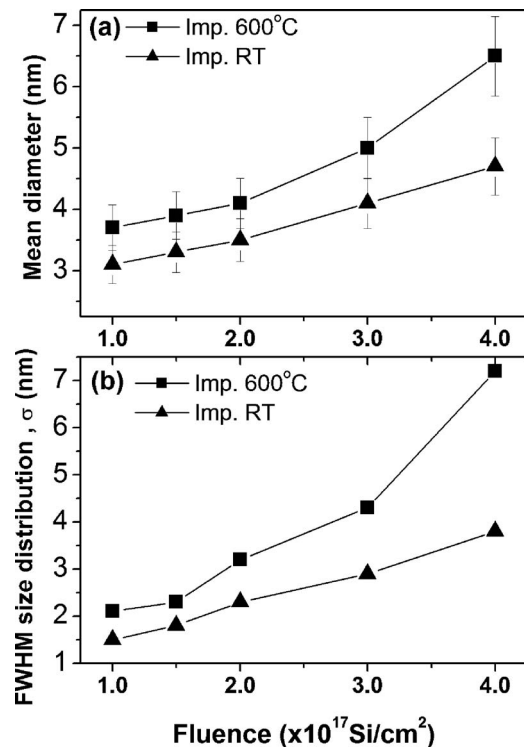


FIG. 5. Results from TEM analyses for samples implanted at RT (triangles) and at 600 °C (squares), annealed at 1100 °C/1 h. (a) Mean diameter of the Si NCs and (b) size distribution as a function of the implantation fluence. The error bar in (a) is 10%.

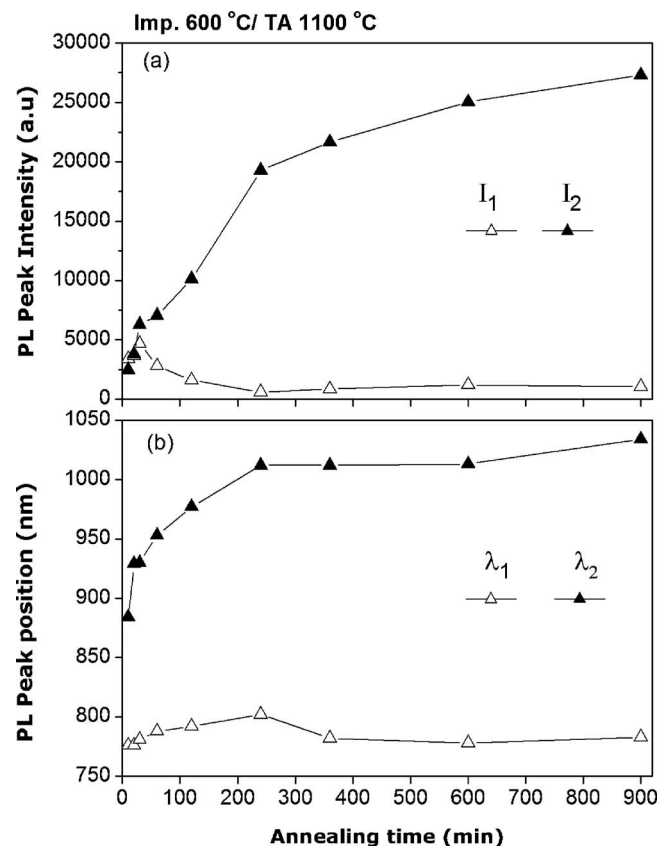


FIG. 6. (a) PL peak intensities and (b) positions as a function of the annealing time at 1100 °C for samples implanted at 600 °C. I_1 and I_2 represent the peak intensities for the short and the long wavelength PL bands centered at the positions λ_1 and λ_2 , respectively.

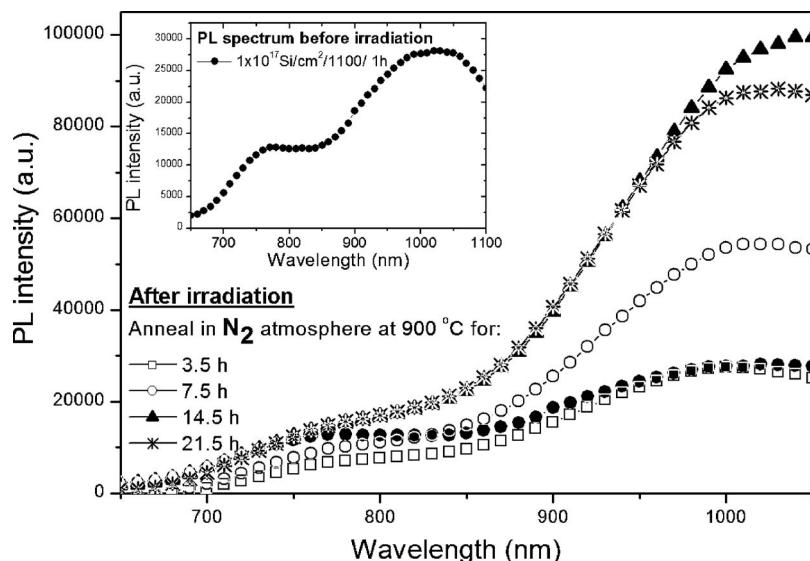


FIG. 7. PL spectrum of the 1.0×10^{17} Si/cm² implanted sample annealed at 1100 °C/1 h (full circle); see the inset. Corresponding PL spectra after irradiation followed by 900 °C anneal in N₂ atmosphere at different times: 3.5 h (open square), 7.5 h (open circle), 14.5 h (full triangle), and 21.5 h (asterisk).

that could recombine radiatively with emitting energies above 1.6 eV ($\lambda < 780$ nm) are captured in these centers, and their emission appears at the same energy of the interface state. We assume that the PL intensity reduction of this short wavelength band by increasing the implantation fluence starts to occur when the recombination energies of carriers are lower than the energy of the radiative interface state.

Regarding the PL band located at the long wavelength side, the PL peak redshift with increasing implantation fluence indicates that its origin is related to quantum confinement effects. In fact, the TEM measurements have shown that the mean size and dispersion of the Si NCs increase with the implantation fluence and with the annealing time. Hot implantations create precursors (prenucleation centers) for the nanocrystals, allowing them to nucleate when submitted at higher temperatures. Consequently, larger and more dispersed NCs are formed when compared to RT implantations, as illustrated by Fig. 5.

The PL intensity reduction observed for the highest implantation fluence in Fig. 2(a) could be explained as follows. The PL cross section for absorption came from the product of the oscillator strength of the transitions and the electronic density of states.²⁵ This product is a function of the size of the NCs, and both terms work in opposite direction as the nanoparticles size changes. Consequently, there is an optimum size for which the emitted PL has a maximum. Then, it is very likely that after certain fluence the optimum size of the distribution overcomes and, consequently, the resulting PL intensity decreases. In addition, we cannot disregard the influence of the Si NCs radiative lifetime, which depends on the nanoparticle size and its interface quality. Larger Si NCs having longer radiative lifetimes²⁵ are also more likely to contain nonradiative recombination centers.¹⁴

Concerning the annealing time dependence of the 1000 nm PL band, it shows a significant PL peak redshift with increasing annealing time (up to 6 h), followed by saturation—see Fig. 6(b). According to quantum confinement effects, this behavior is in agreement with the Si NCs growth with the annealing time, as confirmed by TEM measurements (not shown).

III. INFLUENCE OF THE POSTANNEALING ENVIRONMENT ON THE PL RECOVERY OF ION IRRADIATED SI NCs

A. Experiment

The original Si NCs precipitates were produced following the same procedure described in Sec. II A with a sample implanted with $\Phi = 1.0 \times 10^{17}$ Si/cm². Further, the samples were irradiated with a 2 MeV Si⁺ beam at a fluence of 2.0×10^{13} Si/cm². Under these conditions the original PL emission was completely quenched and the Si NCs were fully amorphized as revealed by TEM experiments (not shown here), while the SiO₂ environment was also damaged.

In a next step the as-irradiated samples were annealed at 900 °C in an atmosphere of N₂ or Ar. As will be described below, the PL emission was recovered, but with different characteristics as compared with the original ones.

For the PL measurements as well as for the TEM observations, we have used the apparatus already described in Sec. II A.

B. Results

1. N₂ annealing atmosphere

In Fig. 7 we display the PL spectrum corresponding to $\Phi = 1.0 \times 10^{17}$ Si/cm² implanted sample further annealed at 1100 °C which shows, as already described, two PL bands. The Si irradiation performed at 2 MeV quenched both PL bands completely. The subsequent annealing performed at 900 °C for 3.5 h brings as a consequence a full recovery of the original long wavelength PL band (open square). The same does not occur with the short wavelength one, where only 40% of the original intensity was restored. Further anneal for 7.5 h increases the PL intensity of the 1000 nm band by almost a factor of 2, but still was not able to reach the original PL intensity of the 780 nm band (open circle). This is only achieved after 14.5 h of annealing time (triangle). Under these conditions the PL intensity of the long wavelength band is more than four times the one corresponding to the original sample. Finally, the annealing performed for

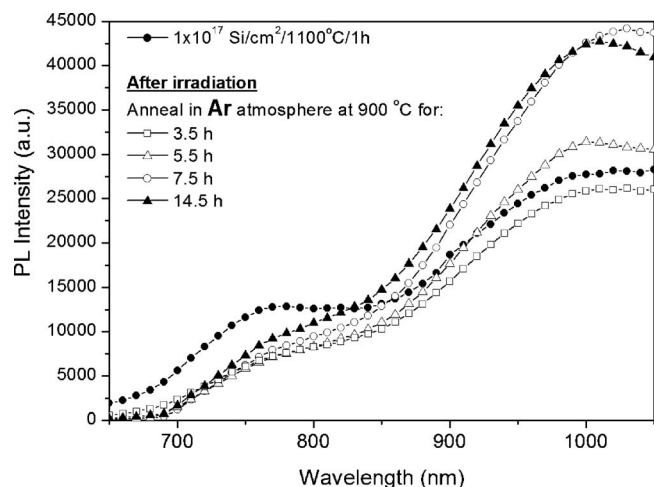


FIG. 8. PL spectrum of the 1.0×10^{17} Si/cm² implanted sample annealed at 1100 °C/1 h (full circle). Corresponding PL spectra after irradiation followed by 900 °C anneal in Ar atmosphere at different times: 3.5 h (open square), 5.5 h (open triangle), 7.5 h (open circle), and 14.5 h (full triangle).

21.5 h shows almost the same results (asterisk) as the ones described above, indicating a saturation effect on the resulting PL intensity.

By fitting both PL bands with Gaussian distributions we were able to observe that their peak positions did not suffer any shift, indicating that the postanaling did not produce any modification in the Si NC distribution. This feature was confirmed by TEM observations (not shown here), which indicate that the mean size of the nanocrystals (3.0 nm) and its distribution (1.6 nm) remains the same as compared to the nonbombarde sample.

In addition, we implanted Si into SiO₂ under the same conditions as described above. Then, we annealed the sample at 900 °C in order to check if at this temperature Si NCs were formed. The results were negative; neither PL emission nor Si NC formation was observed. This means that, after the Si irradiation on the Si NCs, the effect of the 900 °C annealing only induces the recrystallization of the amorphous nanostructures and reconstruction of the surrounding SiO₂ matrix.

2. Ar annealing atmosphere

Figure 8 shows the PL spectrum of the as-implanted at $\Phi = 1 \times 10^{17}$ Si/cm² and 1100 °C anneal sample (full circle). The PL intensity distribution of the Si bombarded sample followed by 3.5 h annealing at 900 °C is also displayed (open square). As can be seen, both PL bands do not reach the original intensity level. Further annealing for 5.5 h (open triangle), 7.5 h (open circle), and 14.5 h (full triangle) indicates an increase of the PL intensity band at 1000 nm with a saturation effect after 7.5 h of annealing time. On the other hand, the original PL intensity of the 780 nm band was never achieved even for longer annealing times.

C. Discussion

First, we will discuss the recovery of the 1000 nm band. As was demonstrated above, the effect of the annealing atmosphere after irradiation consists basically of annealing the damage inside and around the Si NCs. It was already shown

(see Sec. III B) that the annealing at 900 °C does not form Si NCs. On the other hand, it is known that annealing under N₂ or Ar atmosphere induces a release in the interfacial stress at the Si/SiO₂ boundary. Since stress is known to affect the concentration and morphology of defects at the Si/SiO₂ boundary,²⁶ any change in the stress level should influence the PL intensity. Then, concerning the behavior of the 1000 nm band, we attribute the variation of the PL intensity after the 900 °C anneal (in addition to the Si NC recrystallization), to stress relaxation at the Si/SiO₂ interface induced by the annealing atmosphere.

The N₂ or Ar environments produce qualitatively the same effects, but different quantitative results. In fact, under both atmospheres the first annealing performed after 3.5 h reaches or almost reaches the original PL intensity. In addition, in both cases a PL saturation regime is attained. However, we have to point out a major difference. Under N₂ annealing atmosphere the PL saturation intensity is around twice the value reached under the Ar one.

The different behaviors described above can be tentatively explained using the following arguments. As Ar is absolutely inert, an annealing under this atmosphere should only induce a pure thermal relaxation. Therefore, it should only reduce the interfacial stress at the Si NCs-matrix interface and consequently, this effect should influence the PL emission.

On the other hand, although N₂ is considered a relatively inert gas, it has been observed in reaction with Si at moderate temperatures (760–1050 °C) forming ultrathin oxinitride films.²⁷ Moreover, nitride passivation effects on the visible PL from Si NCs have been reported.²⁸ Therefore, as claimed in Ref. 29, the presence of nitrogen contributes to reduce the concentration of interfacial strained Si-O bonds near the interface, bringing as a consequence the nanocrystal surface passivation.

Concerning the PL emission of the 1000 nm band, we can state that the postanaling after irradiation brings beneficial effects by increasing the PL intensity with increasing time. This is due probably to pure stress relaxation in the Ar case and to the same relaxation followed by a surface passivation induced by a thin oxinitride film in the N₂ case, both in addition to the Si NC recrystallization.

Regarding the 780 nm PL band, we have attributed its existence to radiative interfacial states. In this case we observed that, following the Si irradiation and further N₂ annealing, we were able to reach the original PL value only after 14.5 h of annealing time. In contrast, under Ar atmosphere, it never reached the original PL value, independent of the length of annealing time. Then, it is clear for the 780 nm band that 900 °C annealing under Ar or N₂ annealing atmosphere recrystallizes the Si NCs, and rebuilds in an inefficient way the radiative defects existent at the grain-matrix interface. This last feature is revealed by the poor recovery of the PL intensity as compared with the results obtained with the 1000 nm band. With annealing at N₂ ambient, the intensity of the 780 nm band was recovered probably by reconstructing some broken bonds, e.g., the Si=O one. This bond was ascribed in the literature^{4,24,30} to have an important role in the emission due to interfacial states.

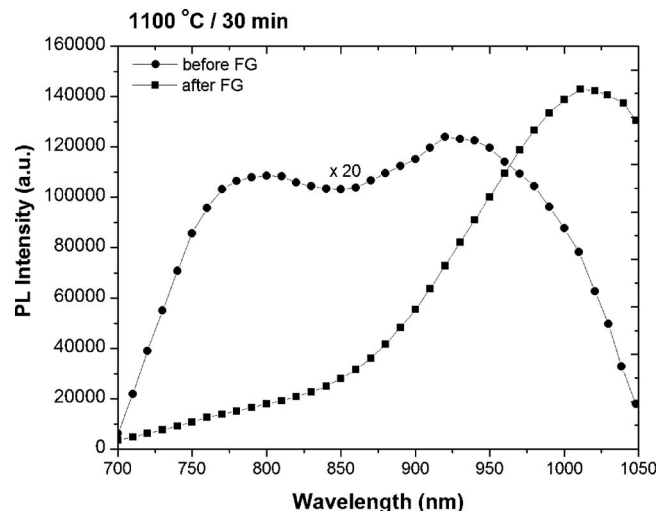


FIG. 9. Typical PL spectra of a sample implanted at 600 °C and annealed at 1100 °C for 30 min before (circle) and after (square) thermal treatment by 1 h at 475 °C in a FG ambient. The PL spectrum before the FG treatment (circle) is multiplied by a factor of 20.

IV. PASSIVATION EFFECT

A. Experiment

In this set of experiments we have used samples implanted with Si ions at 600 °C with a fluence of $\Phi = 1 \times 10^{17}$ Si/cm² into a SiO₂ matrix and further annealed for different time intervals at 1100 °C. Further, these samples were submitted to a passivation process, which consists of a subsequent annealing for 1 h at 475 °C in a forming gas (FG) ambient (mixture of 95% of N₂ and 5% of H₂) at a pressure of 1 atm. Consequently, we have studied the influence of the previous annealing time at 1100 °C on the subsequent FG treatment.

B. Results

Figure 9 displays the PL spectra of a sample preannealed for 30 min at 1100 °C before and after the postannealing performed in a FG ambient. As can be observed, this treatment has a strong effect on the PL shape and intensity. While the short wavelength band (at 780 nm) duplicates its intensity, keeping the position constant, the 1000 nm PL band changes considerably. In fact, its intensity increases by a factor of almost 20, followed by a redshift of about 120 nm.

In this set of experiments we have focused our attention on the long wavelength PL band, since the 780 nm PL one is weakly influenced by the FG treatment.

The results displayed in Figs. 10(a) and 10(b) show the evolution of the maximum PL intensity and peak position before and after the FG treatment, respectively, as a function of the 1100 °C annealing time. The tendency of the PL intensity after passivation is similar to that shown in Fig. 6. It increases up to 120 min of preannealing at 1100 °C and then remains constant. However, the PL signal is considerably higher than the original one.

Regarding the PL peak position, Fig. 1(b) shows the strong redshift induced by the subsequent FG treatment. The PL redshift after passivation is more pronounced for the

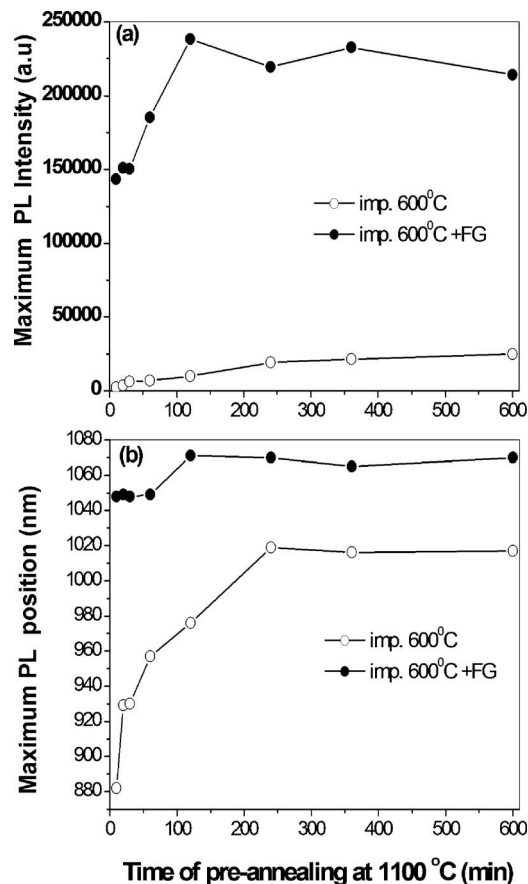


FIG. 10. (a) Maximum PL peak intensity and (b) position as a function of the annealing time at 1100 °C, before (open circle) and after (full circle) passivation process in FG.

shorter annealing times at 1100 °C. For samples annealed for times longer than 200 min the peak position becomes constant.

Figure 11 shows the ratio between the PL intensity of samples after performing the FG treatment and the ones before it. From the figure one can observe the general effect of the passivation process as a function of the PL wavelength for different annealing times at 1100 °C. Two important features should be pointed out: (a) the PL signal is enhanced for the longer wavelength (larger nanocrystals), and (b) the relative PL intensity is higher for the samples annealed for shorter times previous to the passivation. For longer anneals (360 and 600 min) the relative PL intensity becomes very similar.

Finally, it should be stressed that TEM measurements show that the FG treatment does not change the characteristics of the already-formed Si NCs, in agreement with what was observed in previous experiments.³¹

C. Discussion

It was already shown^{18–21,32} that the passivation of non-radiative states and/or defects at the Si NC/matrix interface is an efficient method to increase the PL intensity in Si NCs without changing the original mechanism of PL emission. It was already reported³² that the existence of one free bond, as

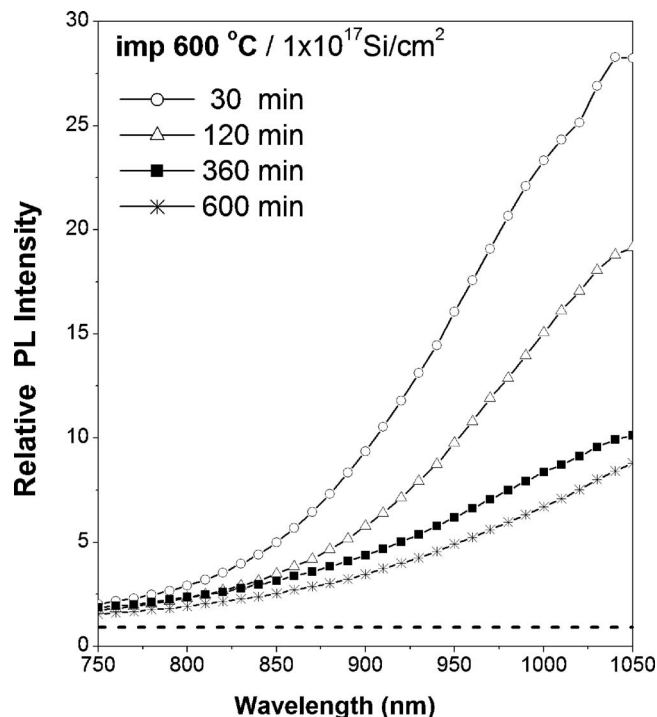


FIG. 11. Relative PL increasing obtained by taking the ratio between the intensity of the PL spectra subsequent and previous to the passivation process of samples implanted at 600 °C and annealed by different times at 1100 °C.

for example the $\cdot\text{Si} \equiv \text{Si}_3$ one, the so-called paramagnetic (P_b) defect center, is already sufficient to quench the PL of the corresponding Si NC.

As displayed in Fig. 9, the FG treatment induces a strong variation in the original PL shape. While the 780 nm PL band is weakly affected, the same does not occur with the long wavelength one. This band not only increases its intensity by a factor of almost 20, but also suffers a strong redshift of around 120 nm. TEM measurements have shown that the FG treatment does not change the characteristic of the Si NCs distribution. Then, it should be concluded that the FG treatment transforms a sizable quantity of large nonradiative nanocrystals in radiative ones.

Since larger nanocrystals have a major surface area as compared to smaller ones, they can present a significant number of defects which, consequently, quench their PL emission. This feature explains why the long wavelength PL band increases its intensity and suffers a strong redshift. In summary, a great number of the larger nonphotoluminescent Si NCs (due to surface defects) start to emit due to the passivation induced by the hydrogen in the forming gas. It should be stressed that the FG anneal does not change the mechanism of the PL emission, which is still of quantum size origin.

On the other hand, it is known that the preannealing at 1100 °C improves the interface quality between the Si NCs and the matrix. As was already reported,¹⁹ there is a direct correlation between the annealing of the nonradiative defects (P_b centers) and the preannealing time. This feature explains the results displayed in Figs. 10 and 11. In fact, the samples implanted at 600 °C, further annealed at 1100 °C without

the FG treatment, continuously increase their PL intensity, presenting a redshift of around 150 nm with an annealing time of 200 min. On the other hand, the subsequent FG treatment shows basically two features: First, the consequent PL emission also depends on the previous annealing time at least up to around 150 min. Second, it is by far more efficient than just a long annealing time performed at high temperature.

V. SUMMARY

It was shown that hot Si implantations into SiO₂ matrix after high-temperature annealing produce two PL bands, one centered at 780 nm and the other at 1000 nm. Then, the present work had three objectives: (a) to investigate the origin of each band; (b) to determine the influence of the post-annealing environment on the recovery of the PL bands after ion irradiation of the Si NCs; and (c) to observe the influence of a FG treatment on each one of the PL bands.

Considering the first objective, by changing the implanted Si fluence and annealing time (at 1100 °C) we arrived at the conclusion that the 780 nm band has its origin in radiative interfacial states since its position was not sensitive to the above-studied parameters. On the other hand, the experimental results indicate that the 1000 nm PL band is related to quantum size effects. This statement is based on the observation of a strong redshift of this band with increasing size of the Si NCs.

The experiments have given some interesting results about the influence of the postannealing environment on the recovery of the PL of ion-irradiated Si NCs: First, the 780 nm PL band was weakly dependent on the kind of environment under which the 900 °C anneal was performed. At most it reaches the original intensity, this recovery being slightly dependent on the kind of atmosphere (N₂ or Ar) used in the experiment. The same was not true for the 1000 nm PL band. The anneal performed in a N₂ atmosphere induces a PL intensity that was almost five times higher than the original one, without changing the PL peak position. Under Ar atmosphere the behavior was qualitatively the same, but, its efficiency was half that achieved using N₂ environment. We have assumed that the recovery in both cases is due to stress relaxation at Si NCs/SiO₂ interface. However, for the N₂ case a passivation due to the formation of very thin oxinitride film could be responsible for the better efficiency observed in the PL recovery.

Finally, we observed that the FG treatment has drastically modified the PL spectrum, affecting considerably the intensity of the long wavelength band and changing its position. This behavior was attributed to the passivation of the defects located at the Si NC surface. Since large nanocrystals have a more extensive surface area, they can contain more defects. So, the passivation process affects preferentially the larger nanocrystals, converting nonphotoluminescent nanocrystals to luminescent ones and, consequently, shifting the peak PL emission to longer wavelengths. Concerning the influence of the annealing time before passivation, it should enhance the surface quality of the Si NCs, eliminating nonradiative defects. This statement is in agreement with the

experimental observation that after passivation the relative PL increase is higher for samples that were submitted to shorter annealing times.

ACKNOWLEDGMENTS

The authors acknowledge FAPERGS, CNPq, and CAPES for the financial support.

- ¹L. T. Canham, *Appl. Phys. Lett.* **57**, 1046 (1990).
- ²Y. Kanemitsu, T. Ogawa, K. Shiraishi, and K. Takeda, *Phys. Rev. B* **48**, 4883 (1993).
- ³T. Shimizu-Iwayama, K. Fujita, S. Nakao, K. Saitoh, T. Fujita, and N. Itoh, *J. Appl. Phys.* **75**, 7779 (1994).
- ⁴L. Pavesi, L. Dal Negro, C. Mazzoleni, G. Franzò, and F. Priolo, *Nature* **408**, 440 (2000).
- ⁵A. T. Fiory and N. M. Ravindra, *J. Electron. Mater.* **32**, 1043 (2003).
- ⁶L. Brus, in *Semiconductors and Semimetals*, edited by D. Lockwood (Academic, New York, 1998), Vol. 49, p. 303.
- ⁷M. L. Brongersma, A. Polman, K. S. Min, E. Boer, T. Tambo, and H. A. Atwater, *Appl. Phys. Lett.* **72**, 2577 (1998).
- ⁸J. Heitmann, F. Müller, L. Yi, and M. Zacharias, *Phys. Rev. B* **69**, 195309 (2004).
- ⁹P. M. Fauchet, *Mater. Today* **8**, 26 (2005).
- ¹⁰T. Shimizu-Iwayama, D. E. Hole, and I. W. Boyd, *J. Phys.: Condens. Matter* **11**, 6595 (1999).
- ¹¹M. Zhu, Y. Han, R. B. Wehrspohn, C. Godet, R. Etemadi, and D. Ballutaud, *J. Appl. Phys.* **83**, 5386 (1998).
- ¹²X. Wu, A. M. Bittner, K. Kern, C. Eggs, and S. Veprek, *Appl. Phys. Lett.* **77**, 645 (2000).
- ¹³B. Garrido Fernandez, M. López, C. García, A. Pérez-Rodríguez, J. R. Morante, C. Bonafos, M. Carrada, and A. Claverie, *J. Appl. Phys.* **91**, 798 (2002).
- ¹⁴S. Cheylan and R. G. Elliman, *Appl. Phys. Lett.* **78**, 1912 (2001).
- ¹⁵G. H. Li, K. Ding, Y. Chen, H. X. Han, and Z. P. Wang, *J. Appl. Phys.* **88**, 1439 (2000).
- ¹⁶U. S. Sias, L. Amaral, M. Behar, H. Boudinov, E. C. Moreira, and E. Ribeiro, *J. Appl. Phys.* **98**, 034312 (2005).
- ¹⁷D. Pacifici, E. C. Moreira, G. Franzò, V. Martorino, F. Priolo, and F. Iacona, *Phys. Rev. B* **65**, 144109 (2002).
- ¹⁸K. S. Min, K. V. Shcheglov, C. M. Yang, H. A. Atwater, M. L. Brongersma, and A. Polman, *Appl. Phys. Lett.* **69**, 2033 (1996).
- ¹⁹M. López, B. Garrido, C. García, P. Pellegrino, A. Pérez-Rodríguez, J. R. Morante, C. Bonafos, M. Carrada, and A. Claverie, *Appl. Phys. Lett.* **80**, 1637 (2002).
- ²⁰S. P. Withrow, C. W. White, A. Meldrum, J. D. Budai, D. M. Hembree, Jr., and J. C. Barbour, *J. Appl. Phys.* **86**, 396 (1999).
- ²¹S. Cheylan and R. G. Elliman, *Appl. Phys. Lett.* **78**, 1225 (2001).
- ²²P. Deák, M. Rosenbauer, M. Stutzmann, J. Weber, and M. S. Brandt, *Phys. Rev. Lett.* **69**, 2531 (1992).
- ²³K. Takeda and K. Shiraishi, *Solid State Commun.* **85**, 301 (1993).
- ²⁴M. V. Wolkin, J. Jorne, P. M. Fauchet, G. Allan, and C. Delerue, *Phys. Rev. Lett.* **82**, 197 (1999).
- ²⁵C. Garcia, B. Garrido, P. Ellegrino, R. Ferre, J. A. Moreno, J. R. Morante, L. Pavesi, and M. Cazzanelli, *Appl. Phys. Lett.* **82**, 1595 (2003).
- ²⁶A. Stesmans, *J. Appl. Phys.* **92**, 1317 (2002).
- ²⁷M. L. Green, T. Sorsch, L. C. Feldman, W. N. Lennard, E. P. Gusev, E. Garfunkel, H. C. Lu, and T. Gustafsson, *Appl. Phys. Lett.* **71**, 2978 (1997).
- ²⁸M.-S. Yang, K.-S. Cho, J.-H. Jhe, S.-Y. Seo, J. H. Shin, K. J. Kim, and D. W. Moon, *Appl. Phys. Lett.* **85**, 3408 (2004).
- ²⁹A. R. Wilkinson and R. G. Elliman, *J. Appl. Phys.* **96**, 4018 (2004).
- ³⁰N. Pauc, V. Calvo, J. Eymery, F. Fournel, and N. Magnea, *Phys. Rev. B* **72**, 205325 (2005).
- ³¹Y. Q. Wang, R. Smirani, and G. G. Ross, *Physica E (Amsterdam)* **23**, 97 (2004).
- ³²M. Lannoo, C. Delerue, and G. Allan, *J. Lumin.* **70**, 170 (1996).